

Early Quaternary sedimentary processes and palaeoenvironments in the central North Sea

RACHEL M. LAMB,^{1*} MADS HUUSE¹ and MARGARET STEWART²

¹School of Earth, Atmospheric and Environmental Sciences, University of Manchester, Oxford Road, Manchester M13 9LP, UK

²The Lyell Centre, British Geological Survey, Research Avenue South, Edinburgh EH14 4AP, UK

Received 30 June 2015; Revised 27 July 2016; Accepted 5 August 2016

ABSTRACT: A number of elongate trough-like features are observed in the early Quaternary succession of the central North Sea basin. A definitive model of formation for the features remains unclear but the troughs may aid in our understanding of the depositional environment of the early Quaternary. In total, 380 troughs were mapped over 11 000 km² using continuous 3D seismic data and analysed in conjunction with well log data and understanding of the probable palaeogeographical context. The troughs were formed in a marine setting on the slope of a large clinoform set during a period of rapid progradation. The geometry and infill of the troughs, as well as the marine setting, strongly support a model of repeated density-driven downslope flows which excavate and then infill the troughs perpendicular to the strike of the slope. A subset of the troughs are observed to form parallel to the strike in such a way that cannot be easily explained by downslope processes alone. A number of possible models are considered for the formation of these along-slope troughs; here we conclude that the most likely scenario involves modification of the downslope flows by currents which divert the features along-slope while maintaining the erosive nature of the flow. Copyright © 2016 The Authors. *Journal of Quaternary Science* Published by John Wiley & Sons Ltd.

KEYWORDS: downslope processes; early Quaternary; North Sea; palaeoenvironment; seismic.

Introduction

The North Sea is a mid- to high-latitude epicontinental sea located between the British, Scandinavian and Northern European landmasses, which is connected to the North Atlantic to the north and the English Channel to the south (Fig. 1). The Norwegian Trench, which runs parallel to the Norwegian coast along the eastern margin of the North Sea, reaches depths of over 700 m; however, the rest of the North Sea averages close to 100 m water depth, gently increasing northward towards the Atlantic margin. The present-day North Sea is dominated by tidal currents creating features such as the large sandbanks and waves in the Southern Bight (Caston and Stride, 1970; McCave, 1971; Terwindt, 1971; Caston, 1972; Otto *et al.*, 1990; Gatliff *et al.*, 1994). Overall, a shallow anticlockwise current system is present currently in the North Sea; water from the North Atlantic flows into the basin from the north-west, around the Shetlands, moving southwards and mixing with both a relatively minor influx of water from the Channel and freshwater input from the northern European and British river systems (Fig. 1; Otto *et al.*, 1990; Svendsen *et al.*, 1991; Turrell *et al.*, 1992; OSPAR, 2000; Gyllencreutz *et al.*, 2006). The mixed water in the southern North Sea returns to flow north and eastwards mixing further with water flux from the Baltic river system in the Skagerrak region, eventually feeding into the Norwegian Channel which forms the main output of water from the North Sea (Fig. 1; Otto *et al.*, 1990; Svendsen *et al.*, 1991; Turrell *et al.*, 1992; OSPAR, 2000; Gyllencreutz *et al.*, 2006).

The Quaternary deposits in the North Sea can be subdivided across the southern, central and northern North Sea depocentres, of which the central North Sea contains more than 1 km of sediment (Caston, 1977; Cameron *et al.*, 1987; Sejrup *et al.*, 1991; Sørensen *et al.*, 1997; Fyfe *et al.*, 2003; Rasmussen *et al.*, 2005; Nielsen *et al.*, 2008; Knox *et al.*, 2010; Anell *et al.*,

2012; Golędowski *et al.*, 2012; Ottesen *et al.*, 2014). The gross stratigraphic architecture can be divided into a Lower Pleistocene deltaic and marine-dominated succession, and a Middle to Upper Pleistocene to Holocene succession dominated by glaciogenic formations (Cameron *et al.*, 1987, 1992; Gatliff *et al.*, 1994; Stoker *et al.*, 2011). These two successions are separated by a regional glacial unconformity that is commonly marked at its base by an expansive network of tunnel valleys (Cameron *et al.*, 1987; Wingfield, 1989, 1990; Gatliff *et al.*, 1994; Praeg, 2003; Stoker *et al.*, 2011; Stewart *et al.*, 2013).

Preliminary work on the lower Quaternary succession was undertaken during comprehensive mapping of the North Sea stratigraphy during the 1980s and 1990s, and relied on relatively widely spaced 2D seismic lines, which were calibrated shallow boreholes up to 250 m deep, and numerous short seabed cores up to 6 m long (Caston, 1977; Holmes, 1977; Stoker *et al.*, 1983; Stoker and Bent, 1985, 1987; Cameron *et al.*, 1987; Sejrup *et al.*, 1987, 1991, 1994; Knudsen and Sejrup, 1993). In the southern North Sea, Middle and Upper Pleistocene glaciogenic deposits are relatively thin; the boreholes and shallow cores were able to penetrate deep into the Lower Pleistocene deltaic and marine sequences, identifying a wide depositional plain from Britain to Denmark that was flooded at the onset of the Quaternary (Cameron *et al.*, 1984, 1989, 1993; Funnell, 1996; McMillan *et al.*, 2005; Rose, 2009), but became subaerially exposed following a marine regression before the Middle Pleistocene (Cameron *et al.*, 1984, 1989, 1993; Funnell, 1996). In the central North Sea, Middle and Upper Pleistocene glaciogenic deposits are much thicker; thus, the boreholes and shallow cores largely penetrate the glaciogenic succession (Stoker and Bent, 1985; Cameron *et al.*, 1987; Sejrup *et al.*, 1987, 1991, 1994; Knudsen and Sejrup, 1993).

This paper uses basin-scale, continuous 3D seismic data to investigate furrowed landforms preserved in the seismic stratigraphy of the early Quaternary succession (Figs 2 and 3). It aims to investigate the process of formation of these landforms, with respect to the likely palaeoenvironment, and

*Correspondence to: R. M. Lamb, as above.
E-mail: rachel.lamb@manchester.ac.uk

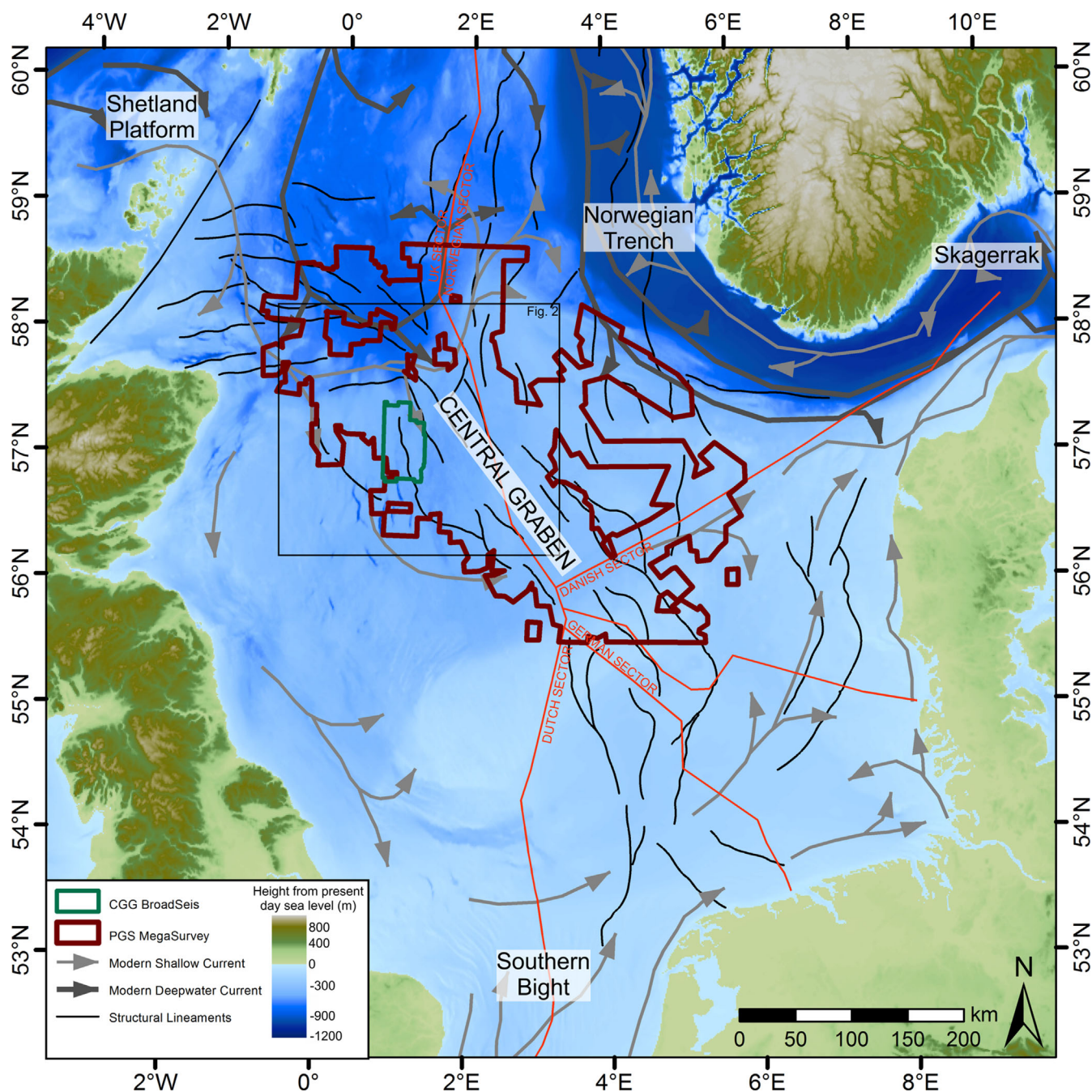


Figure 1. Regional map of the central North Sea showing the extent of the 3D seismic data used in the study, the PGS CNS MegaSurvey and CGG BroadSeis™ surveys, as well as present-day circulation of water currents in the North Sea from OSPAR (2000) with Mesozoic structural lineaments from Ziegler (1992). Bathymetry data from Ryan *et al.* (2009).

propose a model for trough formation. In doing so the paper attempts to further the understanding of the depositional environments of the early Quaternary North Sea basin.

Regional setting

The North Sea originated due to a series of rifting episodes during the late Palaeozoic and Mesozoic eventually culminating in volcanism and rifting in the Mid-Jurassic to Early Cretaceous (Ziegler, 1992). Rifting in the North Sea ceased when the axis of extension shifted to the north-west of Britain, leaving an aborted rift controlling subsidence patterns in the North Sea. The Cenozoic record of the North Sea shows multiple events of basin inversion, subsidence, uplift and erosion throughout the period (Ziegler, 1992; White and Lovell, 1997; Huuse, 2002; Stoker *et al.*, 2005; Anell *et al.*, 2010; Gołędowski *et al.*, 2012). In the Quaternary, thermal subsidence has been the primary

driver of basin development, magnified by rapid infill of the basin allowing for the build-up of the thick Quaternary succession (Huuse, 2002; Anell *et al.*, 2010; Gołędowski *et al.*, 2012).

At the onset of the Quaternary the geometry of the North Sea is considered to have comprised an elongate basin orientated along a NW–SE axis over the Central Graben, extending across the region of the current central North Sea and well into what is now the southern North Sea (Fig. 1; Holmes, 1977; Cameron *et al.*, 1987; Fyfe *et al.*, 2003; Rasmussen *et al.*, 2005; Nielsen *et al.*, 2008; Knox *et al.*, 2010; Anell *et al.*, 2012; Gołędowski *et al.*, 2012; Ottesen *et al.*, 2014). Away from the main NW–SE-trending basin, the remainder of the area which is now the North Sea most likely consisted of a relatively flat plain, subaerially exposed or with either extremely shallow water depths. Infill of the basin during the early Quaternary was rapid, particularly in the southern North Sea, which is noted to be infilled and sub-aerially exposed at some point during the early

Quaternary (Cameron *et al.*, 1984, 1989, 1993; Funnell, 1996). The early Quaternary stratigraphy is represented by the Southern North Sea Deltaic (deltaic to pro-deltaic marine sediments) and Dunwich (non-marine fluvial to inter-tidal sediments) groups, in the southern North Sea, and the Zulu group (deltaic to pro-deltaic sediments) in the central North Sea (Cameron *et al.*, 1992; Gatliff *et al.*, 1994; Stoker *et al.*, 2011). The deltaic sediments in the southern North Sea were sourced primarily from the south-east by the Rhine–Meuse and Baltic river systems (Overeem *et al.*, 2001; Busschers *et al.*, 2007). The overall northerly progression of these sediments is expressed by the preservation of a set of clinofolds – sloping depositional surfaces – that mark the progradation of the early Quaternary delta (Fig. 3).

The early Quaternary saw the onset of global cooling and the initiation of northern hemisphere glaciation (Raymo, 1994; Lisiecki and Raymo, 2005, 2007; Miller *et al.*, 2011), with evidence for ice in the central North Sea thus far restricted to iceberg scours observed within 3D seismic

datasets, and apparently present from the onset of the Pleistocene (Dowdeswell and Ottesen, 2013). Morphological evidence for a shelf-wide, grounded glaciation in the early Quaternary central North Sea remains ambiguous, although highly debated and fragmentary evidence has suggested that there is a possibility for glacial activity in the early Quaternary (Graham *et al.*, 2011, and references therein).

This study focuses on the central third of the central North Sea between 56°30'N and 58°N (Fig. 2). In this area the early Quaternary basin is at its deepest, accumulating up to 1.1 km of sediment (Fig. 3; Caston, 1977; Holmes, 1977; Cameron *et al.*, 1987; Fyfe *et al.*, 2003; Rasmussen *et al.*, 2005; Nielsen *et al.*, 2008; Knox *et al.*, 2010; Anell *et al.*, 2012; Gołędowski *et al.*, 2012; Ottesen *et al.*, 2014). The entire early Quaternary section is located within the Aberdeen Ground Formation of the central North Sea Zulu Group, representing marine and pro-deltaic to deltaic sediments (Fig. 3; Gatliff *et al.*, 1994; Stoker *et al.*, 2011). Dating of the section comes principally from mapping of chronostratigraphic markers from Dutch

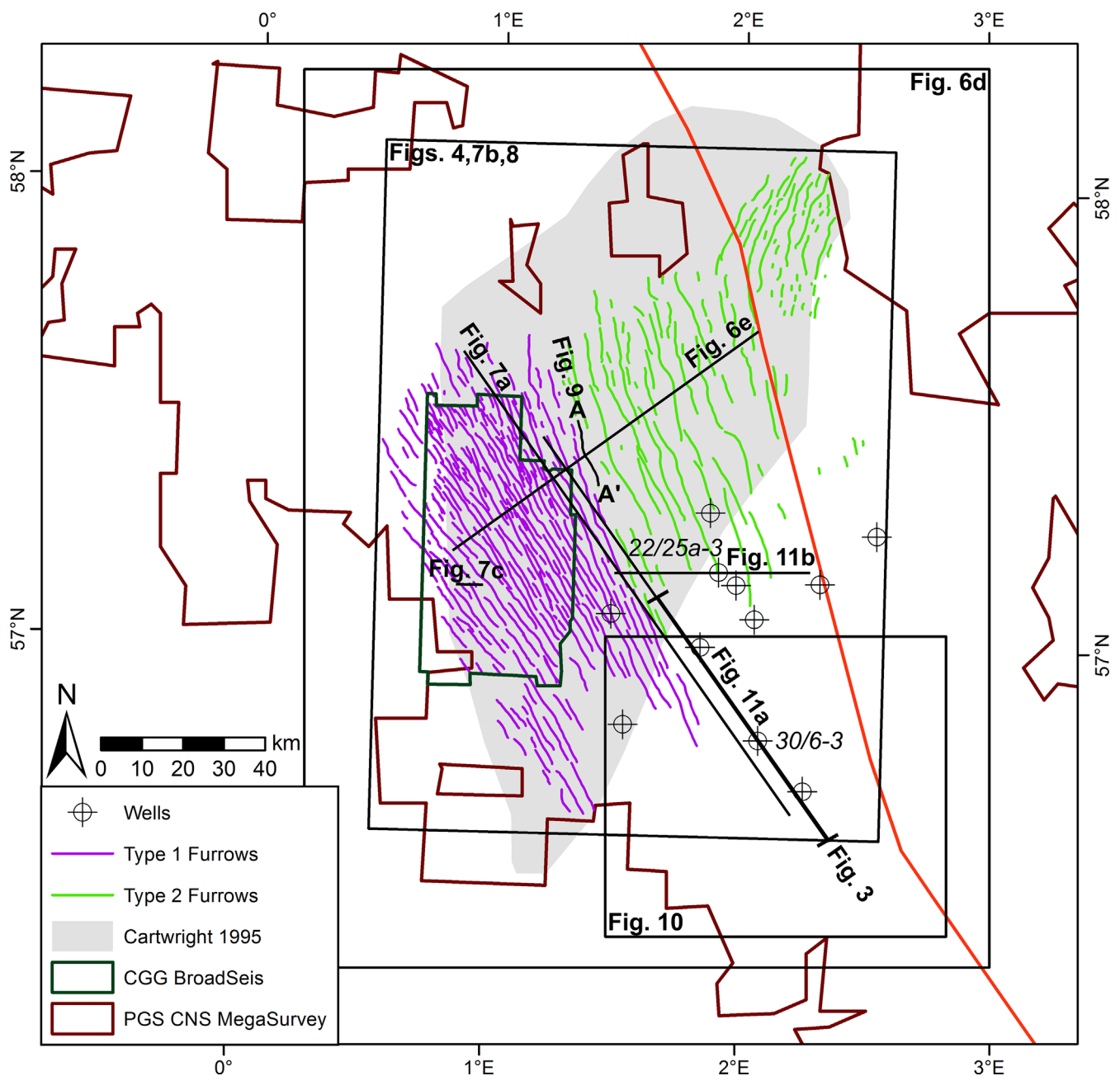


Figure 2. Map showing the mapped thalwegs of the troughs overlying the extent suggested by Cartwright (1995). Locations of Figs 3–11 and wells used in the study are shown. Location is shown in Fig. 1.

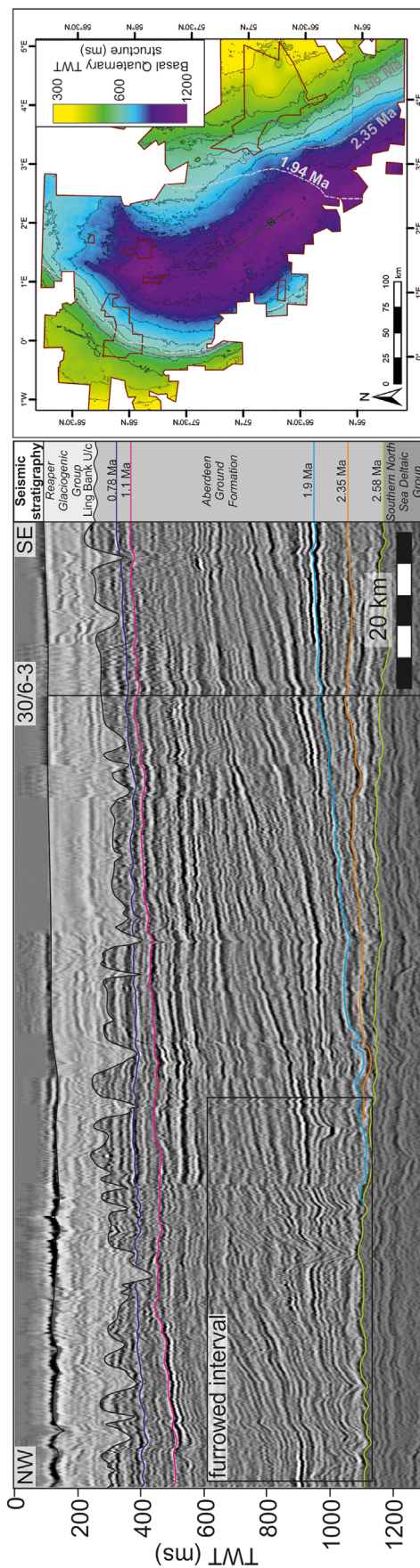


Figure 3. Regional seismic cross-section ($50\times$ vertical exaggeration) showing the regional seismic stratigraphy of the study area identifying the furrowed interval in the Aberdeen Ground Formation of the early Quaternary (based on Cameron *et al.*, 1992; Gatliff *et al.*, 1994; Stoker *et al.*, 2011). Dating of chronostratigraphic horizons from Dutch sector well A15-03 (Kuhlmann *et al.*, 2006) and BGS borehole 77/02 (Stoker *et al.*, 1983). Inset map shows the base Quaternary TWT structure, clinoform breakpoints for 2.58, 2.35 and 1.94 Ma chronostratigraphic ties and location of section. Location of the seismic line is shown in Fig. 2. Seismic data courtesy of PGS.

sector well A15-03 identified by Kuhlmann *et al.* (2006) at 2.58 Ma (base Quaternary), 2.35 Ma and 1.9 Ma through an integration of multiple chronological proxies including biostratigraphy, palaeomagnetism and wireline log data (Figs 2 and 3; Kuhlmann *et al.*, 2006; Noorbergen *et al.*, 2015). Palaeomagnetic data from BGS core 77/02 was also used to provide chronological ties for the Brunhes–Matuyama reversal (0.78 Ma) and the base of the Jaramillo event (1.1 Ma) (Figs 2 and 3; Stoker *et al.*, 1983). The seismic stratigraphy of the earliest Quaternary in this part of the basin shows strong characteristic features in the form of elongate troughs, ‘v’ shaped in cross-section, which run approximately parallel to the basin axis along the basin floor (Figs 3 and 4). These features have been observed in the past (Cartwright, 1995; Knutz, 2010; Kilhams *et al.*, 2011; Buckley, 2012), but a *consensus* has not been reached over the processes which formed them. Understanding the processes involved in the formation of these features could add more detail to palaeo-environmental reconstructions of the early Quaternary North Sea.

Data and methods

Data used for this study include two 3D seismic cubes: the PGS CNS MegaSurvey (v. 2012), with an area of 88 000 km², and the CGG BroadSeisTM seismic cube covering an area of 2250 km² (Figs 1 and 2). The MegaSurvey resolves to 10–15 m vertically with horizontal bin spacing of 50 m while the BroadSeisTM survey resolves to 7–8 m vertically with bin spacing of 12.5 m. To complement the seismic data, 11 wells were selected towards the south-east of the study area to identify any patterns in the sediment grain size distribution. All depth conversions from ms TWT to metres assume a standard seismic velocity of 1800–2000 m s⁻¹.

The seismic stratigraphy of the furrowed area was mapped using a semi-automated mapping methodology to separate the troughs in time. Two reference horizons corresponding to the chronostratigraphic ties from the southern North Sea at 2.58 and 1.94 Ma were mapped carefully across the area and then imported into the *Paleoscan* software which builds a 3D geo-model based on the seismic and reference horizons and extracts a horizon stack automatically. Comparison of these semi-automated horizons to the original seismic can be used to quality control the result, allowing for minor editing of horizons before key horizons are selected for analysis and interpretation. Thickness maps and clinoform breakpoints for each of the horizons were made to understand the evolution of the basin during the formation of the troughs.

Individual troughs were identified firstly in time slice using a combination of seismic amplitude and the variance attribute (Fig. 4). Locations, orientation and extent of each furrow were noted before full mapping occurred in cross-section, using time-slices to ensure accurate correlation between each line. In cross-section troughs were mapped from the basal truncation upwards identifying the sides of the troughs based on the curvature of the reflections and truncations (Fig. 5). Acoustic anomalies, namely velocity pull-up effects, were observed and noted. Pull-ups generally occur when a contrast in sediment type causes the velocity of the seismic wave to increase with respect to the background sediment, causing the underlying seismic reflections to appear mounded, and can be linked to consolidated deposits in an otherwise unconsolidated sediment.

Each trough was mapped individually in both the regional and the broadband seismic datasets with the boundaries and thalwegs digitized as polygons then exported to GIS software to extract length, average width, depth, sinuosity and orientation. The difference in orientation between the furrows and the clinoform slope was

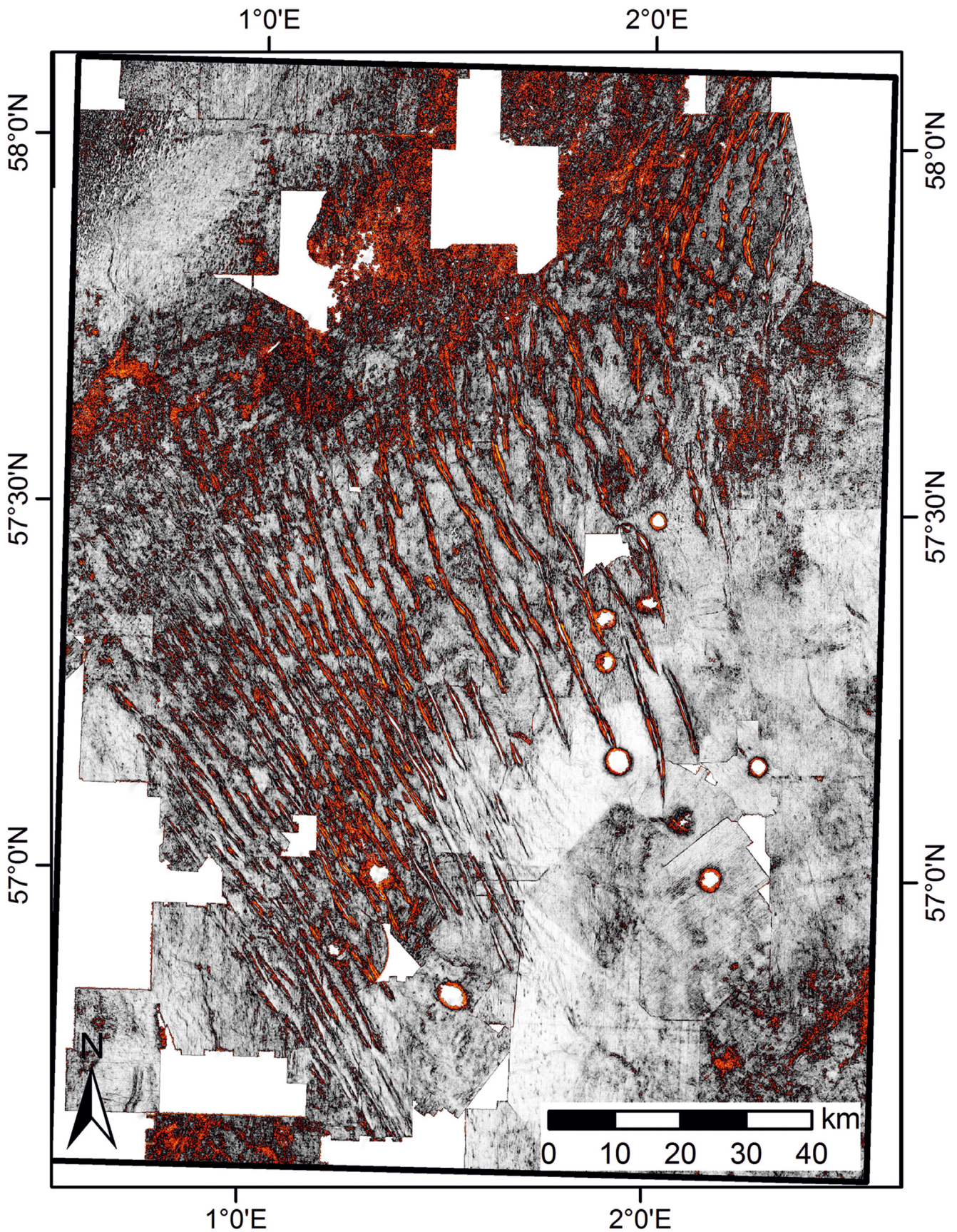


Figure 4. Extraction of amplitude variance from a 10-ms TWT window either side of the F04 horizon, demonstrating the full extent of the troughs and highlighting the individual troughs used in mapping. Location is given in Fig. 2.

calculated by splitting the clinoform break point for the 1.94-Ma horizon, which corresponds to the earliest stage of trough formation, into six sections (Fig. 6). The average strike of the clinoform slope was found for each section

and then the difference between each trough and the nearest section of the clinoform was calculated. This allowed the change in orientation of the troughs relative to the clinoforms from west to east to be quantified.

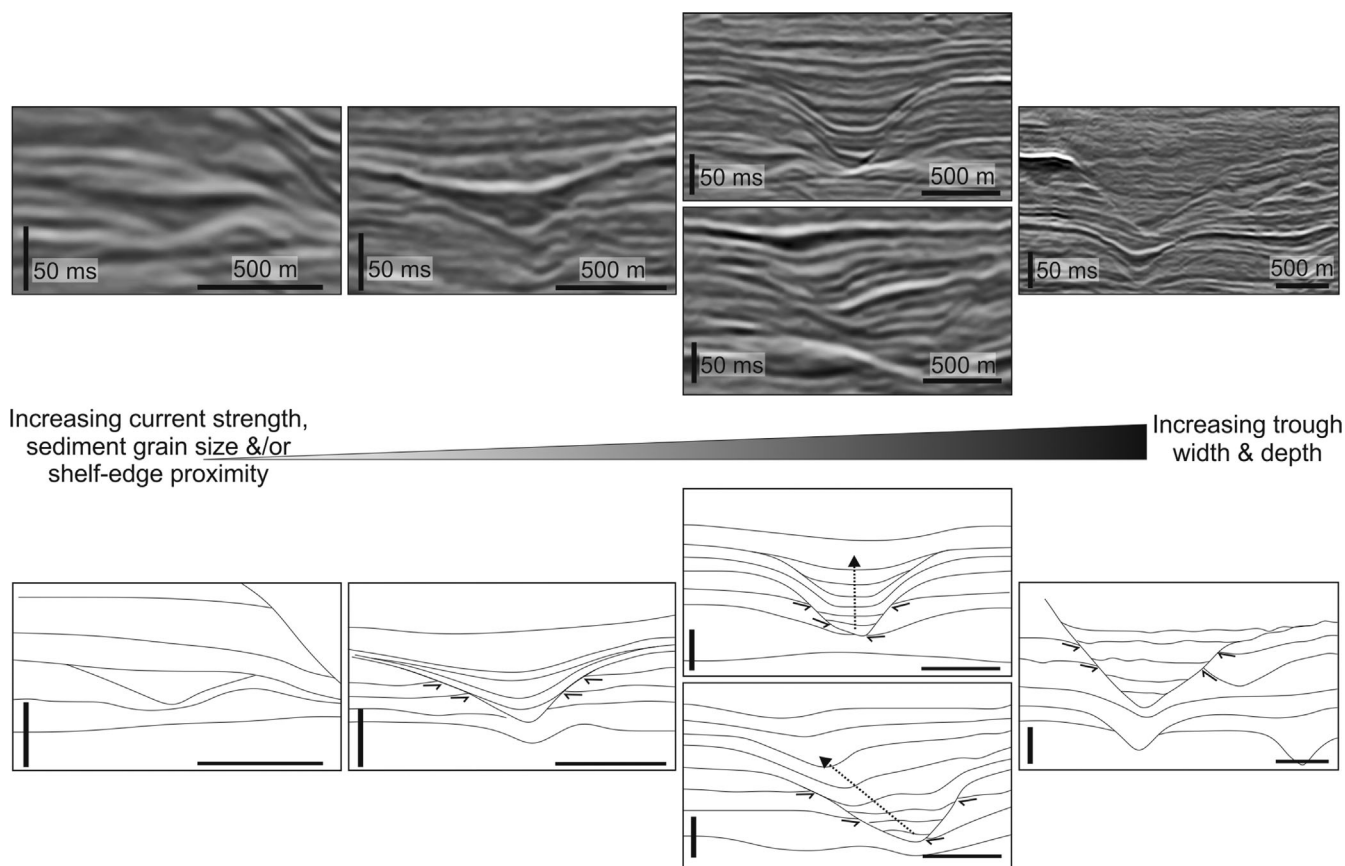


Figure 5. Diagram of cross-sectional form of troughs indicating spectrum of forms observed. Forms grow in width and depth with increasing current velocity, sediment grain size or proximity to the shelf breakpoint.

The available well data consist primarily of gamma log data and lithological descriptions from well cuttings which were depth converted using pre-calibrated time–depth curves provided by TGS. Wells are used to interpret the grain size distribution and facies.

Results

A total of 380 troughs were mapped across the study area, revealing a lens-shaped ‘furrowed’ interval (Figs 7 2 and 8) covering a total area of approximately 12 000 km² contained within an up to 0.5-km-thick succession (Figs 3 and 7). The troughs are elongated and slightly sinuous in planform and vary between ‘u’ and ‘v’ shaped in cross-section with sizes from 0.1 to 50 km in length, 0.1 to 3 km in width and 30 to 275 ms TWT (or 27 to 250 m) deep. Each trough was separated based on plan-form type, cross-sectional form and horizon attributes to compare features and unlock clues to potential modes of formation. The results presented here first discuss the characteristics of the troughs in planform, cross-section and longitudinal profile before looking at the separation of troughs by horizon and the analysis of the background sedimentation through well logs.

Plan form

In plan form the troughs can be divided into two distinct types separated by size and differences in orientation relative to the clinoforms of the basin infill. Figure 6 shows the width/depth ratio of the two types, and the angular difference between the axis of the troughs and the strike of the clinoform slope. Type 1 troughs are almost perfectly perpendicular to the strike of the clinoforms (Fig. 6b). Type 2 troughs have a wider range of orientations but are, on average,

approximately parallel to the clinoform strike (Fig. 6c). There is significant overlap between the overall size of type 1 and type 2 troughs, but type 2 troughs are generally wider and deeper than type 1 (Fig. 6a,e).

The two types of trough identified here in planform are geographically separate and each covers approximately half the total furrowed area (Fig. 6d,e). There are 266 type 1 troughs (70% of the total) found in the west of the furrowed area, while type 2 troughs dominate the eastern half with 114 in total (30%). Type 1 troughs have a higher density in distribution and distances between individual troughs lie between 0 and 5 km but most commonly fall between 1 and 2.5 km (Fig. 6d,e). Type 2 troughs show distances of 1.5–8 km between them, but on average are more than 2.5 km apart (Fig. 6d,e). Type 1 troughs are the only furrows that exhibit signs of lateral migration; this effect appears to be limited to troughs located on the most western margin of the basin (Figs 5 and 8).

Cross-sectional form

The characteristics of the troughs in cross-section are defined by the basal truncation, infill character, stacking pattern and size. The cross-sectional forms displayed in the troughs occur on a spectrum from extremely small ‘proto-trough’ features <5 km long, <1 km wide and <50 ms (~45 m) deep to extremely large troughs with strong basal reflectors which reach 2–3.5 km in width and 250 ms (~225 m) deep. Both type 1 and type 2 troughs exhibit this spectrum, which is summarized in Fig. 5.

The smallest, ‘proto-troughs’ tend to be ‘v’ shaped with poorly defined basal truncations and simple infill patterns which are at or below seismic resolution, leaving onlap of only a single reflector onto the truncated background

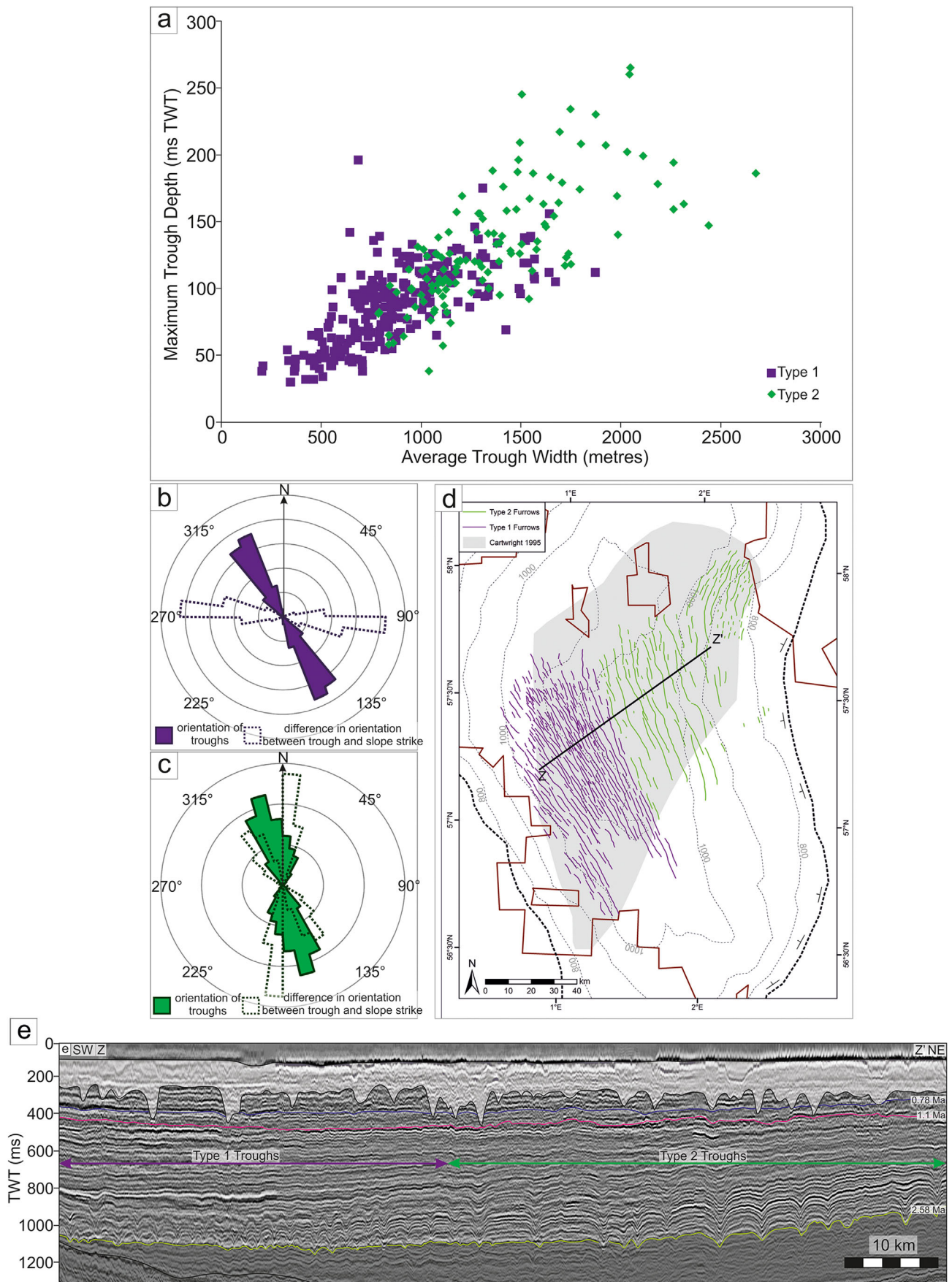


Figure 6. (a) Graph of average width versus maximum depth of troughs by trough type indicating the trend towards type 2 troughs being wider and deeper than type 1. (b,c) Rose diagrams indicating the bidirectional orientation of type 1 and 2 troughs as well as the angular difference between the orientation of the troughs and the strike of the closest section of the clinoform slope. (d) Map showing the position of type 1 and 2 troughs relative to the 1.94-Ma clinoform break point as well as strike direction indicators for the active clinoform. For location refer to Fig. 2. (e) Seismic section across the axis of the basin showing the distribution of type 1 and type 2 troughs in cross-section. Note the high density of type 1 troughs and the thicker deposits of type 2. For location of section see Fig. 2. Seismic data courtesy of PGS.

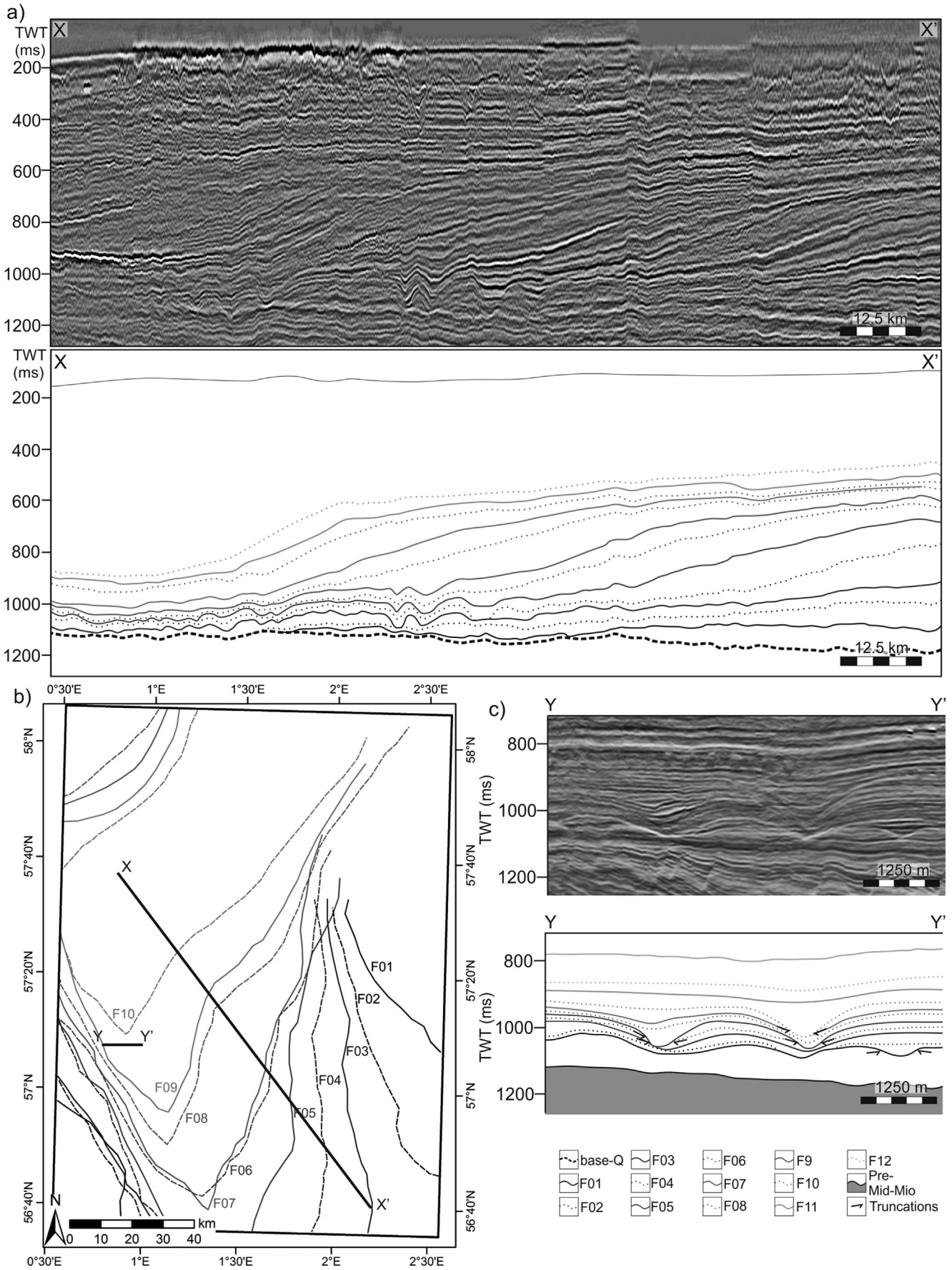


Figure 7. (a) Seismic section identifying the mapped horizons and clinoform progradation. Seismic section courtesy of PGS. (b) Map indicating approximate progression of the clinoform break points through time. (c) High-resolution seismic section showing incision of troughs from different horizons. Seismic data courtesy of CGG. For locations refer to Fig. 2.

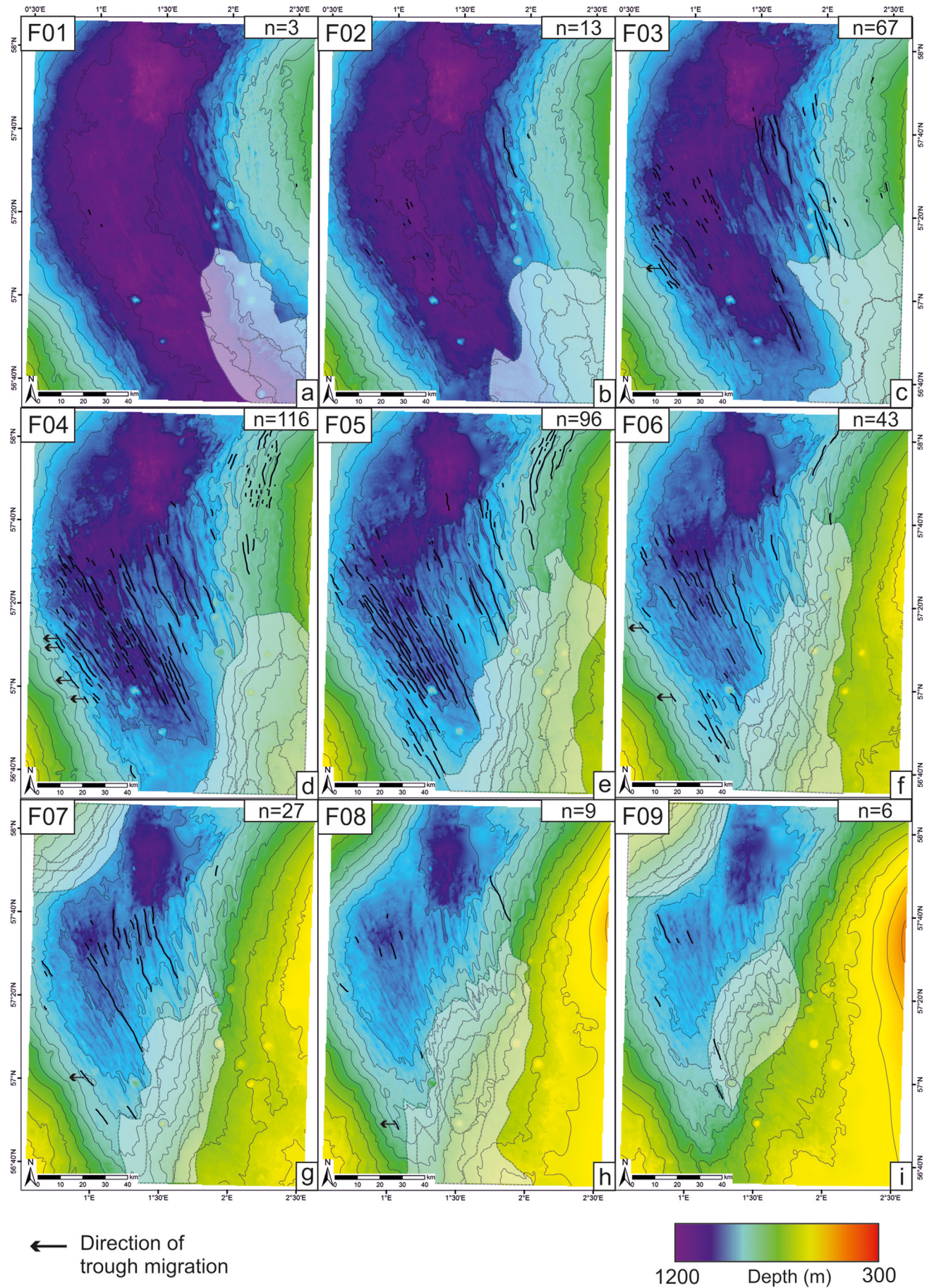


Figure 8. Series of depth maps showing the structural trends of the basin during the furrowed interval. Each map shows depth to named horizon and 50-m contours (black). Grey area is depocentre, based on thickness maps, from named horizon to horizon below with the exception of F01, which represents the depocentre from base Quaternary to F01 horizon. Grey dashed contours represent the thickness contours of the depocentre every 30m. Maps are overlain by the troughs which incise from that horizon. For location refer to Fig. 2.

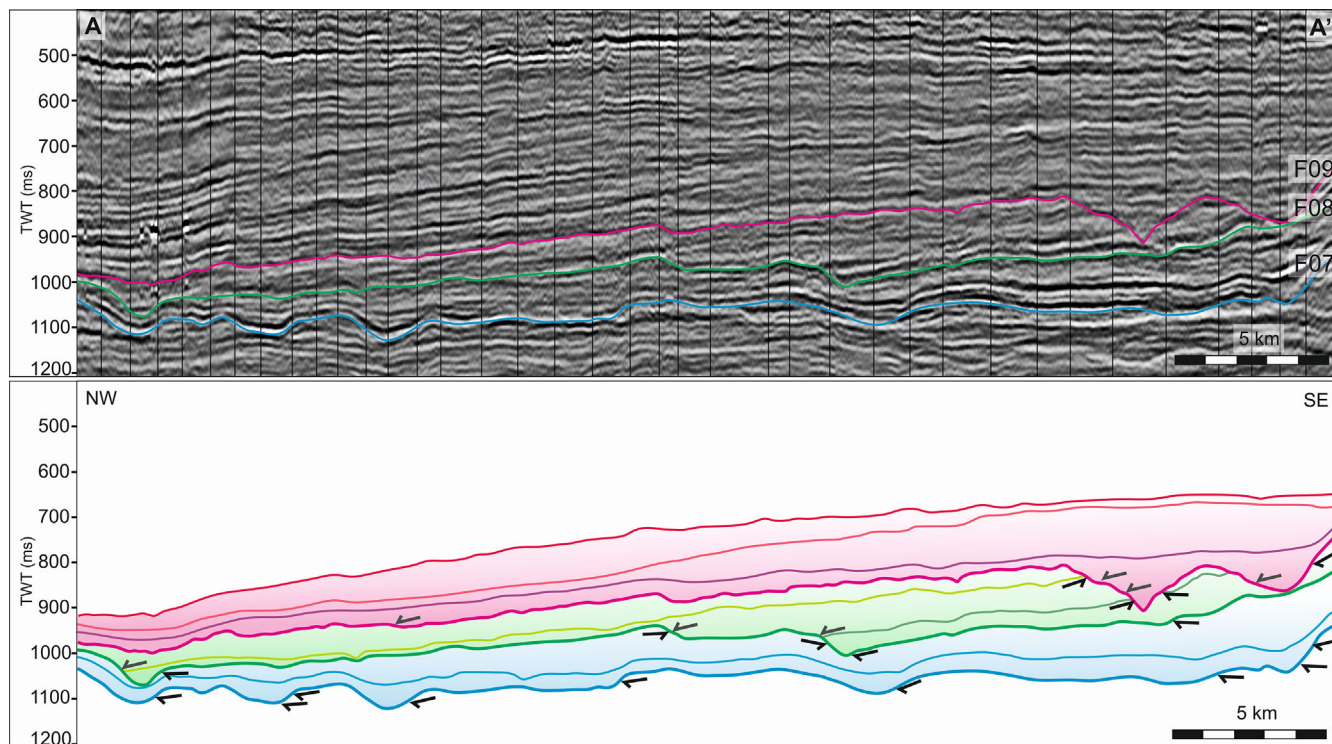


Figure 9. Long profile A–A' of trough showing repeated pulses of active furrowing as well as highlighting periodicity of truncations along base of active furrow. Location is given in Fig. 2. Seismic data courtesy of PGS.

sedimentation (Fig. 5a). Troughs with this cross-sectional form only exhibit this form and do not generally persist to be expressed on the next seismic reflection. These troughs are shorter in length than all other troughs.

As both width and depth of the troughs increase the basal truncation becomes increasingly well-defined and the sedimentary package below the troughs starts to exhibit velocity pull-up effects (Fig. 5b). Infill patterns tend to become better defined and in most of the troughs are aggradational in nature (Fig. 5b,c). Seismic stacking patterns vary between reflectors which onlap the basal truncation of the trough and more 'draped' reflectors in which the reflectors can be seen to merge with the background sedimentation (Fig. 5b,c). A repeated pattern of truncation followed by onlap followed by 'drape' can be seen within individual troughs over 100 ms (90 m) deep (Fig. 5c). The cross-section of the troughs may change along the axial length of the trough as the width and depth of the trough varies. A small minority of troughs (2.5%) exhibit asymmetrical stacking patterns indicative of lateral migration (Fig. 5d).

The largest troughs, over 1.5 km wide, exhibit only an aggradational, onlapping stacking pattern which is usually near-horizontal and sub-parallel (Fig. 5e) unlike smaller troughs in which on-lapping reflectors tend to follow the shape of the basal truncation (Fig. 5b–d). The largest troughs are also the youngest and tend towards shorter axial lengths. Troughs with this cross-sectional form do not exhibit any other cross-sectional form.

Longitudinal profile

With the exception of the proto-troughs all troughs persist after initial formation and are expressed on numerous horizons before being fully infilled. If horizons are taken to be time-synchronous events (Mitchum *et al.*, 1977a,b) then a relative timeline can be formed of the length of time each trough is active for. Troughs are expressed on up to three horizons after their formation (Fig. 8) and, although type 2

troughs have generally thicker deposits than type 1 (Fig. 6), there is no significant difference between the lengths of time individual troughs were active for.

Individual trough fills show thickness variations along the length of the trough. Long profiles of the troughs (Fig. 9) reveal an undulating thalweg as well as a pattern of repeated truncation. Over-deepening of the thalwegs along the trough axis commonly occurs every 3.5–6 km with clear basal truncations (Fig. 9). Between over-deepenings truncations are less clear and the seismic reflections between the trough and the background sedimentation appear more conformable (Fig. 9). Between one and three instances of repeated truncation into the trough infill, which is also observed in cross-section, occurs during the lifetime of most of the troughs (Fig. 9) showing the same undulating thalweg. This, along with the cross-sectional form, yields a cut-and-fill geometry to the troughs.

Horizon mapping

Ten horizons, F01–F10, were chosen from the semi-automated mapping to define the furrowed interval as well as the chronostratigraphic ties (Fig. 7). Of these ten horizons, troughs were incised into nine, F01–F09. The horizons show the present-day TWT structure, whereas thickness maps between horizons are used as a proxy for the palaeo-depocentre (Fig. 8) and basin and slope contours (Fig. 7).

The basal Quaternary surface is identified at the base of the furrowed interval and the TWT-structure defines a basin elongated along a NW–SE axis which roughly follows the underlying Mesozoic Central Graben until approximately 57° 30'N when the basin begins to deviate eastward from the graben trend eventually resulting in a north-easterly orientation (Figs 3 and 7). The furrowed area spans the width of the basin covering ~12 000 km² in the deepest part of the basin. No troughs originate from the base Quaternary horizon, but instead furrowing was initiated almost immediately above with some troughs penetrating into the base Quaternary surface from a higher level. The onset of furrowing coincides

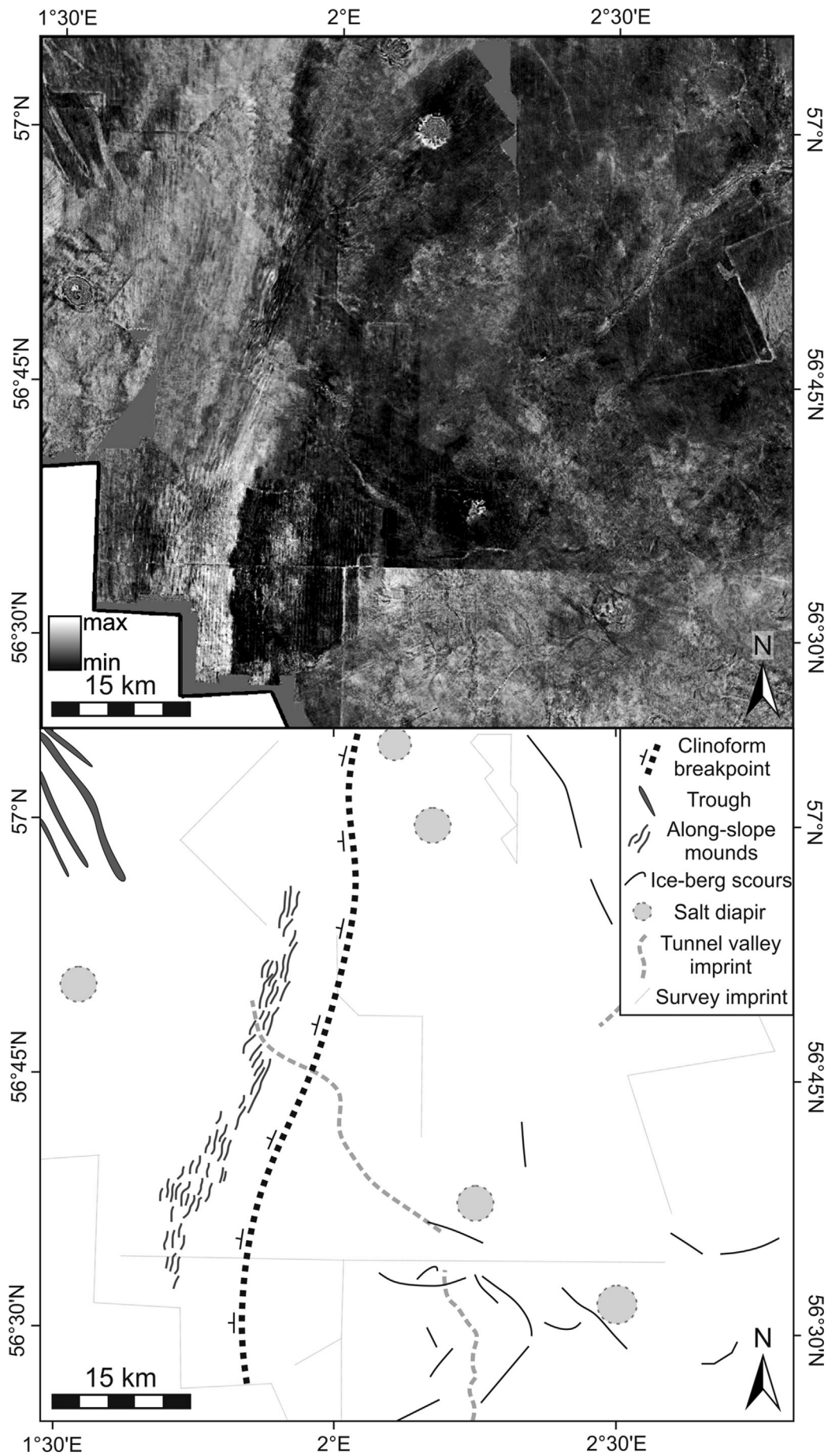


Figure 10. Exact amplitude extraction slice of F04 horizon with sketch interpretation identifying clinoform breakpoint and slope direction indicators as well as mounded features found on the slope of the clinoform sub-parallel to slope contours and iceberg scours marks observed on clinoform top sets. Location is shown in Fig. 2.

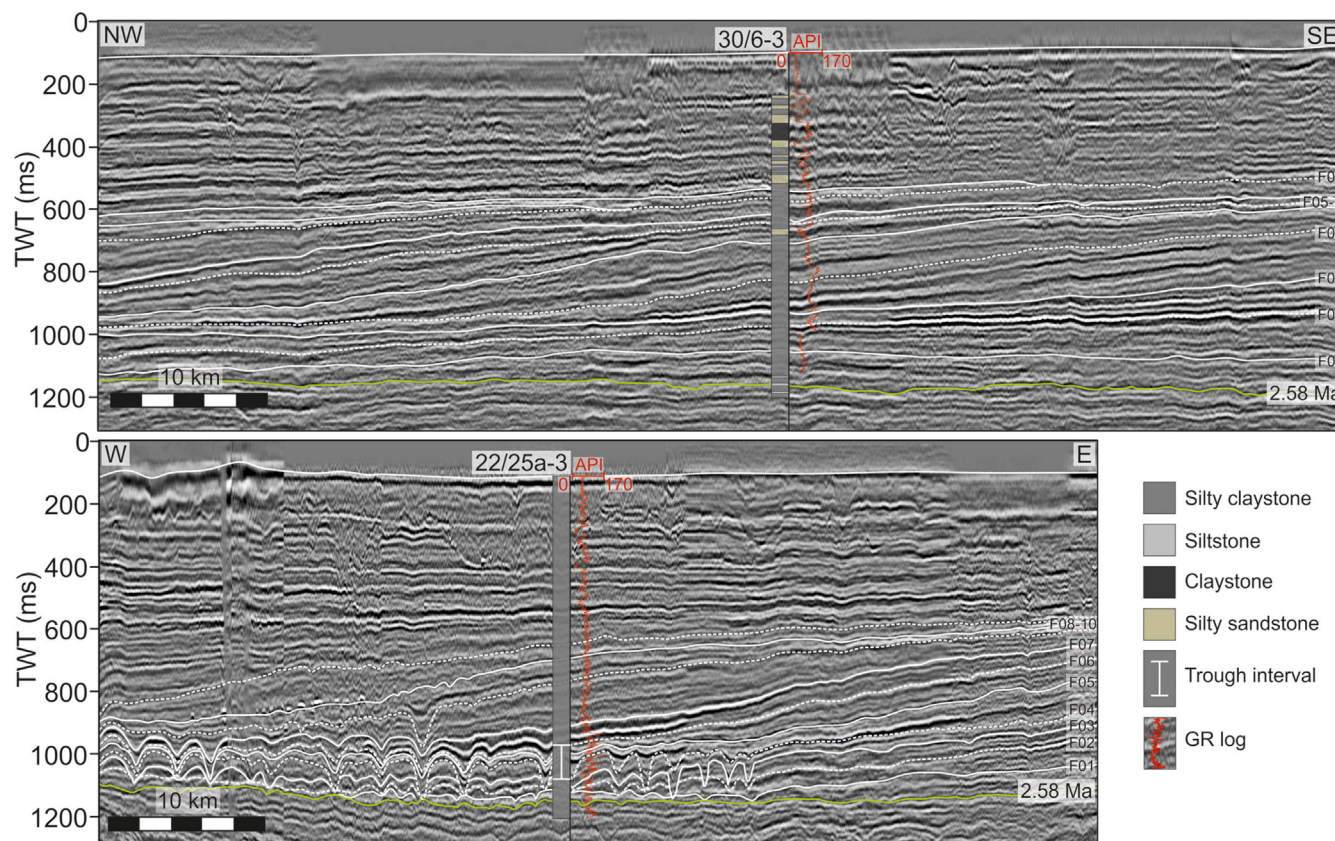


Figure 11. Well correlation panels for wells 30/6-3 and 22/25a-3 correlating gamma log response, lithological descriptions and seismic data for the background sedimentation within the furrowed interval (30/6-3) and the sedimentation within the infill of the trough (22/25a-3). Location is given on Fig. 2. Seismic data courtesy of PGS, and well data courtesy of TGS.

with the F01 surface. Initially most troughs are small, but quickly increase in size and frequency up to a peak of trough activity at horizon F04 before a steady decay in the number and spread of new troughs (Fig. 9).

From the earliest Quaternary onwards most of the sedimentation comes from the south-east as a large prograding delta, expressed by a distinctive clinoform set, moved northwards to fill in the basin (Figs 3, 7 and 9). Clinoform heights (the sloping depositional surface between the shelf-break and the basin floor) can be used as a proxy of water depth at any given time. Although clinoform heights vary between the F01 and F09 surfaces, the range consistently falls within 300–400 ms TWT (Figs 3 and 7) which approximates to between 270 and 360 m water depth. All horizons show some input from the southern delta system, but in the F06–F07 and F08–F09 intervals there is a secondary input from the north-west (Fig. 8g,i). By the F09 surface, the clinoform breakpoint has prograded over 200 km, resulting in a dramatic change in basin shape, with the axis of the basin lying on a new NE–SW axis (Figs 7b and 8i). The basin south of 57°30'N is almost completely filled in by F09, although clinoform heights do not drop below ~250 m (Fig. 7a), indicating continued deeper water in the migrating basin centre. By the time of the F09 surface, the furrowed area no longer straddles the deepest part of the basin, instead being on the southern margin of the basin, incising into the clinoform slope to just downslope of the breakpoint. No channel systems are observed on the topsets of the clinoforms in the seismic stratigraphy from F01 to F10, but iceberg scours and small slope-parallel mounded features are observed (Fig. 10).

Well correlation

Eleven wells with gamma-ray logs and lithological descriptions from well cuttings were used to investigate the

background sedimentation and trough infill. Wells 22/25a-3 and 30/6-3 are found to be representative of the section and so best describe both trough infill and background sedimentation (Fig. 11) with well 22/25a-3 penetrating a type 2 trough and well 30/6-3 representing an undisturbed section through the background sedimentation.

The principal background sedimentation in the furrowed section was silty-claystone as seen from the lithological descriptions of well 30/6-3 (Fig. 11). Towards the base of the furrowed section and thus the base Quaternary, 30/6-3 shows the presence of thin silt layers, which unfortunately are not recorded in the gamma-ray log due to a gap in the data. The gamma-ray log shows numerous peaks but maintains the relatively high response expected from claystone throughout the furrowed section. The exception to this is a drop in the gamma response between horizons F05 and F06 which corresponds to the presence of a thin (<20 m) bed of silty sandstone in the lithological description. This bed corresponds to the topset of a prograding clinoform which onlaps the basin margin to the north-west. In the shallower section above the furrowed interval there is a switch from dominantly silty claystone to silty sandstone.

Well 22/25a-3 shows the same dominant silty claystone lithology which is consistent throughout the whole section. The trough that 22/25a-3 penetrates does not appear, from the lithological descriptions, to have any effect on the sediment of the fill. In comparison, the gamma-ray log shows some distinction between the trough and the background sedimentation, generally showing a higher and more variable gamma response, but still within the typical responses of claystones (60–150 API; Rider, 2002). The higher response and isolated peaks together suggests a fining of the material within the fill of the trough.

Discussion

Palaeogeographical setting

Previous studies of the troughs have inferred variable ages and models of formation without coming to a *consensus*. Models suggested by Cartwright (1995), Knutz (2010) and Kilhams *et al.* (2011) invoke a variety of marine processes, from solely downslope processes to bottom-currents, while Buckley (2012) inferred a subglacial origin. To understand the processes involved in the formation of the troughs the palaeogeographical setting must be considered.

Mapping of the basin at the onset of the Quaternary and the onset of the furrowing reveals an epeiric marine basin with water depths up to 400 m (Figs 3 and 7; Cameron *et al.*, 1984, 1989, 1993; Funnell, 1996; Ottesen *et al.*, 2014). The Aberdeen Ground Formation is described as marine in nature, and associated lithological descriptions and gamma-ray logs from the wells indicate background sedimentation is fine silts and clays (Fig. 11), in agreement with descriptions from the shallower portions of the Aberdeen Ground Formation (Stoker and Bent, 1985, 1987; Cameron *et al.*, 1987; Knudsen and Sejrup, 1993). Well 30/6-3 shows a coarsening-upwards sequence with input of silty sandstones towards the top of the section (Fig. 11). The presence of iceberg scours on the clinoforms confirms periodical glacial environments on the margins of the basin.

The North Sea is only considered to have been fully glaciated since the Elsterian, after the basin was filled (<0.5 Ma; Graham *et al.*, 2011), and the subglacial processes inferred to have carved out the troughs (i.e. tunnel valley formation; Buckley, 2012) would rely on pressurized meltwater flow beneath extensive grounded ice sheets (Huuse and Lykke-Andersen, 2000). Tunnel valleys are noted to usually incise into near-horizontal sediments (Huuse and Lykke-Andersen, 2000). As the troughs considered here formed approximately 1.8–2.5 Ma on clinoform surfaces in water depths up to 300 m, a subglacial origin is considered unlikely. Given the palaeogeographical setting (submarine) and the palaeo-glaciological history of the basin, we infer that a submarine origin of the troughs is most likely, in common with previous interpretations (Cartwright, 1995; Knutz, 2010; Kilhams *et al.*, 2011).

The early Quaternary marine basin is elongate and both narrows and shallows towards the north leaving a small, shallow lip over which water could flow into and out of the basin connecting to the North Atlantic (Fig. 3; Cameron *et al.*, 1987; Ottesen *et al.*, 2014). The shape and geometry of the basin is vastly different from the present-day marine basin, limiting any comparisons to the present-day tidally driven circulation system. In terms of overall geometry of the basin, the earliest Quaternary basin appears similar to the early Cenozoic North Sea, with the alignment of areas of greater water depth and the axis of the older Mesozoic Central Graben (Fyfe *et al.*, 2003; Rasmussen *et al.*, 2005; Knox *et al.*, 2010; Anell *et al.*, 2012; Gołdowski *et al.*, 2012). The current system in the earliest Quaternary of the central North Sea is considered a hybrid of the present-day and early Cenozoic; inflow and outflow of water would come primarily through the narrow sill from the northern North Sea and, ultimately, the North Atlantic. Significant sources of fresh water from the Baltic and NW European rivers, as well as partially glaciated catchments in Britain and Norway, are likely to have been more dominant than in the present-day system.

The primary infill of the basin, and thus inflow of fresh water, comes from the south, creating the large deltaic clinoform geometries observed in the seismic data (Figs 3 and 7). This

infill is likely to have been sourced primarily from the Rhine–Meuse and Baltic river systems, which, during the earliest part of the Quaternary, fed into the southern North Sea (Bijlsma, 1981; Overeem *et al.*, 2001; Busschers *et al.*, 2007). The rapid (200 km in approximately 1 Ma) northward progradation of the delta (Figs 3 and 7) suggests a strong northwards flow of water and sediment over the topsets. The northern input of sediment is comparatively sparse and thus, perhaps, a much weaker contribution in terms of water inflow (Fig. 8).

Trough geometry and infill

The geometry of type 1 troughs orientated perpendicular to clinoform strike, with low sinuosity and with repeated cycles of basal truncation and infill, is strongly indicative of downslope processes. The size, geometry and repeated instances of ‘cut-and-fill’ observed in the repeated truncations are all consistent with slope gullies on continental shelves (Shepard, 1965; Field *et al.*, 1999; Stow and Mayall, 2000; Spinelli and Field, 2001).

Slope gullies, such as those found on the Californian continental slope (Field *et al.*, 1999; Spinelli and Field, 2001), have been described as relatively straight, subparallel, downslope-trending features without tributaries or distributaries (Shepard, 1965; Field *et al.*, 1999; Spinelli and Field, 2001). Slope gullies are found on the continental slope commonly extending 10–15 km down slope (Spinelli and Field, 2001) and have been observed to have a spacing of 200–500 m between individual gullies (Field *et al.*, 1999). In a compilation of width versus depth measurements for slope features, Stow and Mayall (2000) found gullies to be within the region of 200–1000 m wide and up to 100 m deep. Although the troughs in this study are deeper than most slope gullies (up to 250 m deep) all other features of their geometry fall within the range of slope gully features.

The basal truncation of the troughs is consistent with down-slope features formed by periodic density-driven flows. Material is carried down the slope in high-density flows dominated by traction processes eroding a series of troughs into the clinoform slope (Syvitski, 1989; Pratson *et al.*, 1994; Cartwright, 1995; Field *et al.*, 1999; Mulder *et al.*, 2003; Mulder, 2011). The exact nature of these flows, whether they are hyperpycnal, turbidity or gravity flows, is unclear; differentiation between the three types is probably only possible from core as the well log data do not show indications of either fining or coarsening within the trough interval (Fig. 11; Mulder, 2011). Hydraulic jumping of high-density flows has been observed where slope changes, particularly gradient, and is the probable cause of the observed periodic over-deepening of the trough thalweg (Komar, 1971; Weirich, 1988; Garcia and Parker, 1989; Mulder, 2011). These interpretations are held out by the infill of the troughs. After basal truncation the infill is consistently structure-less or on-lapping the sides of the troughs which are likely to be axial deposits laid down as the turbidity current wanes allowing for deposition in the base of the trough (Shepard, 1981; Pratson *et al.*, 1994; Field *et al.*, 1999; Mulder, 2011). The ‘drape’ fill that follows is correlative with the background sedimentation of the clinoforms indicative of a more steady-state deposition, probably settling of sediment from suspension. Repeated occurrences of truncation into the infill itself follow the same pattern and the diachronous incision of troughs from different horizons implies repeated turbidity flows reoccupying troughs or causing flow to switch from one trough to a new one.

The troughs are consistently found on the downslope side of the clinoform breakpoint, in agreement with other

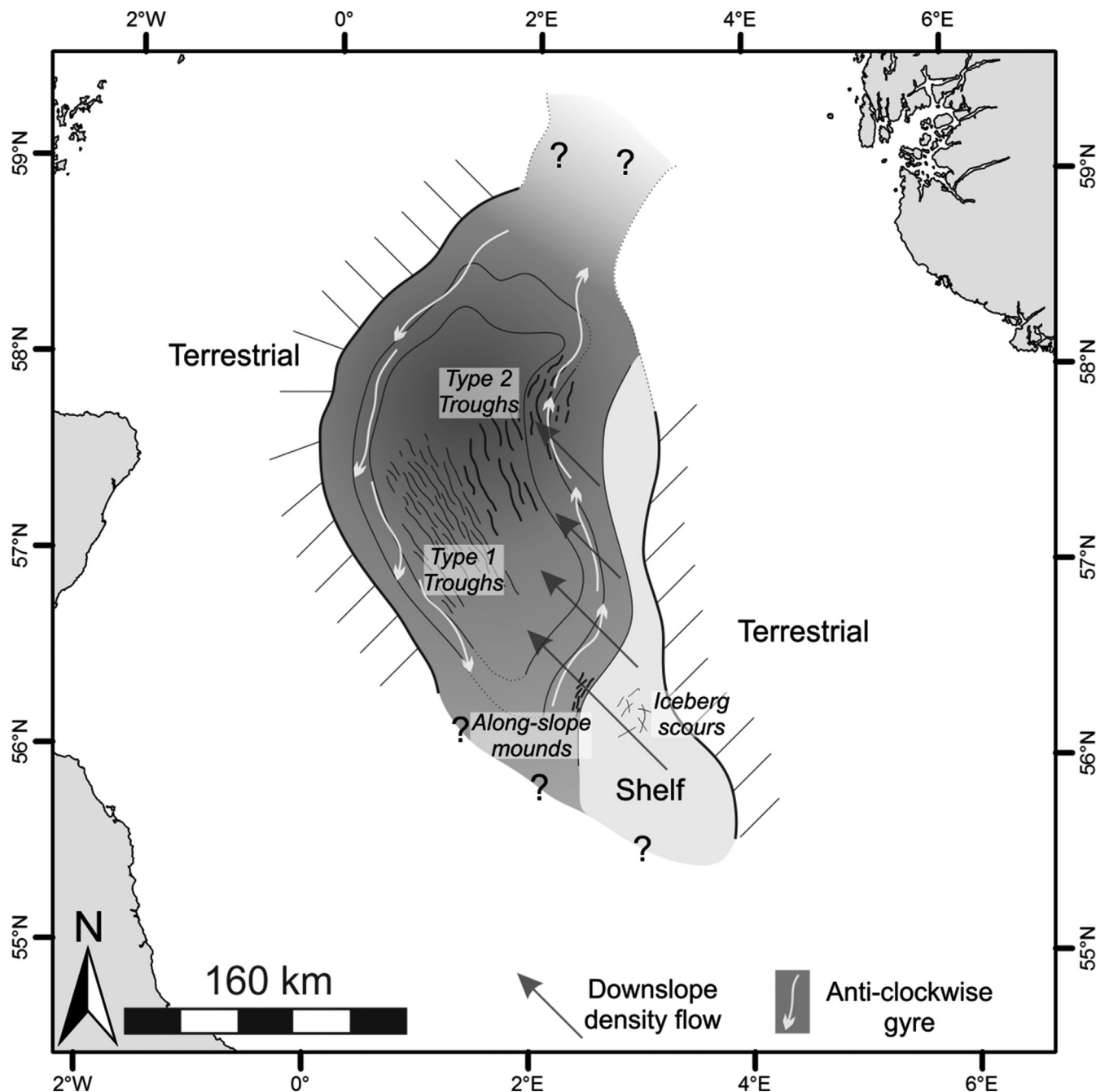


Figure 12. Palaeogeographical reconstruction of the early Quaternary basin and the marine current system identifying anticlockwise circulation of shallow currents and strong downslope processes. The location of shelf and shoreline was estimated from F05 and F06 horizons. The reconstruction is based on results of this study and Cameron *et al.* (1987), Huuse (2002) and Stuart and Huuse (2012).

downslope features particularly slope gullies which rarely truncate the breakpoint (Shepard, 1965; Spinelli and Field, 2001). Troughs initially form at some distance to the slope, probably eroding headwards as has been observed in other downslope features (Pratson and Coakley, 1996; Spinelli and Field, 2001; Harris and Whiteway, 2011) towards the breakpoint. The high abundance of the smaller proto-troughs on horizons F01–F03, in which the distance between the troughs and the clinoform slope was large (in the region of 100 km), is suggestive of either weak initial currents at the onset of furrowing or very distal deposits of a large turbidity current. However, if it is the latter the question arises why, in this particular case, the troughs only begin to erode the background sediments at such a large distance from the slope and why there are no troughs at all further south than 56°30'N. There is not enough evidence in the stratigraphic sequence to make any clear conclusions on why this is the case.

Finally, the similarity between the background sedimentation and the infill of the troughs observed in the well data clearly suggests the trough beds and fills are formed of the same material. The gamma response in well 22/25a-3 shows a more variable and slight fining of the sediment, indicative of a reworking of the background sediment into giant channelized bedforms discussed herein (Fig. 11).

It is concluded here that the downslope-orientated type 1 troughs are formed by downslope gravity processes in the form of regular density-driven flows which erode the troughs and then infill them (Fig. 12). Their overall geomorphology both in cross-section and in long-profile, orientation and infill agree with this model of formation. The along-slope-orientated scours (type 2), while sharing many characteristics with type 1 troughs, require an additional process to explain their along-slope aspect. This is considered below.

Deviation of troughs

The increase in trough size and the change in orientation towards the eastern side of the basin (type 2 troughs) are not easily explained by downslope processes alone. Although lateral variations in downslope features are observed elsewhere, for example along the margin of Equatorial Guinea (Jobe *et al.*, 2011) and the margin of New Jersey (Pratson *et al.*, 1994), these are often controlled by sediment supply or the shape of the basin (Shepard, 1965; Field *et al.*, 1999; Stow and Mayall, 2000; Spinelli and Field, 2001; Jobe *et al.*, 2011). In the early Quaternary, the basin depocentre is consistently observed towards the centre or western side of the basin, suggesting that this area was the area of maximum sediment input, and away from the type 2 troughs to the east (Fig. 8). Thus, it would be expected that lower sedimentation rates towards the east of the basin should limit the size of the type 2 troughs in comparison with the type 1. In virtually all examples of slope gullies and downslope canyons, changes in the orientation of the features follow the shape of the basin, maintaining the features as perpendicular to the strike of the slope (Pratson *et al.*, 1994; Field *et al.*, 1999; Spinelli and Field, 2001; Harris and Whiteway, 2011). Thus, if the type 2 troughs were controlled mainly by downslope currents, they should be seen to deflect westwards down the slope of the eastern margin rather than eastwards along it (Fig. 6).

There are several possible explanations for the deviation of type 2 troughs although the majority can be considered in two main controls: structural controls, such as subsidence or tectonic activity, or sedimentary controls, in the form of additional sedimentary processes. These are considered below.

The primary driving of subsidence in the North Sea during the late Cenozoic is from sediment loading; large quantities of sediment are deposited into the basin during this time, particularly in the southern part of the basin (Huuse, 2002; Anell *et al.*, 2010; Gołdowski *et al.*, 2012). Any differential subsidence due to an unequal load would be expected to have a north–south trend due to the excess loading in the south, although accurately modelling this without extensive decompaction and backstripping calculations is beyond the scope of this paper. The pattern of trough deviation observed in the data does not fit with a N–S loading trend.

Zechstein salt forms most of the salt tectonic complexes in the North Sea. While extensive deformation occurs in the southern North Sea, salt in the central North Sea is observed largely as infrequent salt diapirs (Huuse and Clausen, 2001). Although diapirs have been noted to cause deviation of flow previously (Shepard, 1981; Gee *et al.*, 2007; Wynn *et al.*, 2007) there is no clear correlation in the distribution of diapirs and the troughs. Looking particularly at the type 2 troughs there are no diapirs in close correlation with the troughs which could cause the consistent divergence observed (Fig. 9). On the basis of these two analyses neither subsidence patterns nor salt tectonism can be directly applied to type 2 troughs and a structural control is considered unlikely.

The present-day North Sea has a strong tidal influence and, in the past, observations of contourites suggest bottom-current activity within the late Mesozoic and early Cenozoic. Both of these sedimentary processes could have formed the type 2 troughs as both are known to create along-slope features. However, there is little evidence for either the large tidal bar complexes of the present-day North Sea (Caston and Stride, 1970; McCave, 1971; Terwindt, 1971; Caston, 1972; Otto *et al.*, 1990; Gatliff *et al.*, 1994) or the contourites of the early Cenozoic North Sea (Huuse *et al.*, 2001; Huuse and Clausen, 2001; Galloway, 2002; Rundberg and Eidvin, 2005; Esmerode *et al.*, 2008; Stuart and Huuse, 2012) within the

early Quaternary. Although along-slope features are observed (Fig. 10; Andresen *et al.*, 2008; Stuart and Huuse, 2012) they are an order of magnitude smaller than the troughs. Additionally, any sedimentary process, such as bottom currents, could be expected to be reflected in a change in the infill of the type 2 troughs, either in the structure or in the lithology. The cross-sectional form of each individual trough is not observed to be determined by the type of trough, and well log data show no evidence of lithological change barring a slight fining of material. On this basis it is considered that a completely separate sedimentary process is unlikely to be the cause of the type 2 deviation. However, it is possible that a process may have modified the downslope currents such that the nature of the flow was not drastically changed but the flow direction was, thus limiting any change in the infill character.

Modification of downslope processes

It is therefore proposed that, although downslope processes from the southern clinofolds remain dominant, the type 2 troughs were modified by a secondary process in the form of along-slope currents. Mounded features orientated along-slope have been observed previously in the North Sea during the Miocene to Pliocene and earliest Quaternary (Fig. 10; Andresen *et al.*, 2008; Stuart and Huuse, 2012). The along-slope features have been interpreted to result from an anticlockwise gyre system. Similarly, the present-day circulation of water in the North Sea also has an anticlockwise aspect in which water from the North Atlantic flows southwards along the western margin and mixes with North Sea and river waters in the south, eventually flowing northward along the eastern basin margin (Fig. 1; Otto *et al.*, 1990; OSPAR, 2000). In addition to this, many elongate basins globally show some form of rotational circulation pattern, and fjord circulation in particular is probably the closest comparison to the North Sea; the early Quaternary basin is elongate, with only a comparatively narrow connection to the open ocean and the basin is at least seasonally glaciomarine as evidenced from the presence of iceberg scours (Fig. 10). Fjords have stratified water columns which, in conjunction with the Coriolis force, control strong rotational circulation systems (Syvitski, 1989). Thus, the north-eastward deviation of type 2 troughs in the eastern part of the early Pleistocene depocentre may result from such an anticlockwise gyre.

Along the eastern margin of the basin the periodic gravity-driven currents are proposed to have flowed northwards off the main clinofold slope with gravity encouraging them to divert towards the west. However the anticlockwise gyre on the eastern margin flowed north-east. The two currents mix and interact, changing and lowering the density of the downslope flows. The changed density contrasts with the background water column and the flow no longer penetrates to the basin floor, instead flowing along the contours of the basin slope in the same way that bottom currents flowing out of the Mediterranean Sea at the Straits of Gibraltar flow along the continental slope (Faugères *et al.*, 1984) as well as mesopycnal flows form in stratified water columns (Mulder and Alexander, 2001; Mulder *et al.*, 2003). The mixed flow maintains its velocity due to the additional force of the along-slope current, and traction continues causing erosion of the background sediment forming the slope of the clinofolds in much the same way as the type 1 troughs. The larger scale of the eastward-deflected bedforms (Fig. 6) may be due to a combination of greater current strength relative to sedimentation rate and persistence of the gyre system between gravity flow events. This combination of the flow may explain why

the two types of trough appear on a spectrum in terms of size; as the troughs transition from west to east the flow direction of the gyre increasingly complements and enhances the downslope flows.

Due to their increased size and the change in orientation relative to the clinoform slope, type 2 troughs are considered downslope features modified by along-slope currents (Fig. 12).

Limitations of the model

Limitations to the model of downslope trough formation are considered below.

- **The infill patterns** of the type 1 and type 2 trough do not appear to be significantly different. While the continued dominance of downslope flows is considered the driving mechanism behind furrow formation, changes in infill would be expected due to the effect of current modification on the type 2 furrows. Note that the apparent lack of observed infill difference may not be resolvable in the seismic data, and information from well logs is widely spaced and also may not capture any differences.
- **The effect of up-slope migration**, which may also be expected due to the interaction of the downslope gravity current and the proposed shallow along-slope current, is also not observed. The Coriolis force, in the northern hemisphere, would be expected to deflect northward-flowing currents to the east, resulting in type 2 troughs migrating up-slope, which is not observed. On the western margin of the furrowed area, a small number of asymmetrical troughs do migrate up-slope, suggesting that a southward-flowing gyre, which would be deflected to the west, is determining the migration of the troughs (as opposed to the dominant northwards downslope currents).
- **Feeder systems** for the downslope system are not observed on any of the mapped clinoform topsets, despite a relatively good understanding of such systems of channel/delta systems well into the southern North Sea (Cameron *et al.*, 1989, 1993; Funnell, 1996; Overeem *et al.*, 2001; Rasmussen *et al.*, 2005; Noorbergen *et al.*, 2015). The topsets of the clinoforms are seen in the seismic data (Figs 3, 7 and 11); the clearly visible preserved iceberg scours imply that significant erosion has not occurred – but there remains little evidence for feeder channels as would be expected. A lack of observed feeder channels makes understanding the trigger of downslope flows forming the troughs more difficult. It is noted here that the clinoforms observed in the study area are primarily mud-dominated, with little evidence for coarser deltaic sediments reaching so far north, perhaps suggesting that sediment plumes rather than direct feeder channels are responsible for their build up.

Conclusions

Mapping of 380 trough-like features hosted within a large-scale progradational succession in the central North Sea has been undertaken to build a model for their formation and so further the understanding of the depositional system of the early Quaternary in the North Sea. The troughs were found to be unevenly distributed across the basin and are split into two types based on size and orientation relative to the strike of the clinoform slope. Type 1 troughs are smaller and orientated perpendicular to clinoform strike and were found to be distributed on the western side of the basin, while type 2 are larger and orientated almost parallel to clinoform strike on the eastern side of the basin.

The palaeogeographical setting and the geometry of the troughs strongly supports a model of incision and deposition by downslope processes. Regular but episodic high-density flows carved out the troughs with waning flows allowing the deposition of axial sediments and eventual infill from background sedimentation. Repeated flows reoccupied troughs, leading to a build-up of the cut-and-fill architecture. The differences between type 1 and type 2 troughs, primarily the deviation of the type 2 troughs, cannot be solely explained by lateral variations in downslope processes. A variety of models that may have caused the deviation are considered; we postulate that the most likely scenario involves modification of the downslope flow features in which the nature of the flow is maintained but the direction of the current is deflected along-slope instead of down. The model proposed infers an anticlockwise gyre system creating a flow of water north-eastwards, interacting with the downslope flows, and changing the density of the flow causing it to deviate along the contours of the slope. Questions remain regarding the exact nature of the density-driven flows and their trigger, which are likely only to be resolved by the retrieval of core material from the clinoforms and trough fills.

Acknowledgements. We acknowledge NERC studentship (No: A87604X) and BUFI in conjunction with Forewind for supporting this work, PGS for providing the CNS MegaSurveys, CGG for providing the BroadSeis™ survey, and TGS for providing well data through their Facies Map Browser. Thanks to Schlumberger for the donation of the *Petrel* software and Eliis for the *Paleoscan* software. We would like to thank Martyn Stoker for a very thorough and helpful review which ultimately led to a greatly improved paper.

References

- Andresen KJ, Huuse M, Clausen OR. 2008. Morphology and distribution of Oligocene and Miocene pockmarks in the Danish North Sea – implications for bottom current activity and fluid migration. *Basin Research* **20**: 445–466.
- Anell I, Thybo H, Rasmussen E. 2012. A synthesis of Cenozoic sedimentation in the North Sea. *Basin Research* **24**: 154–179.
- Anell I, Thybo H, Stratford W. 2010. Relating Cenozoic North Sea sediments to topography in southern Norway: the interplay between tectonics and climate. *Earth and Planetary Science Letters* **300**: 19–32.
- Bijlsma S. 1981. Fluvial sedimentation from the Fennoscandian area into the North-West European basin during the late Cenozoic. *Geologie en Mijnbouw*: 337–345.
- Buckley FA. 2012. An Early Pleistocene grounded ice sheet in the Central North Sea. In *Glaciogenic Reservoirs and Hydrocarbon Systems*, Huuse M, Redfern J, Le Heron DP, Dixon RJ, Moscarillo A, Craig J (eds). Geological Society: London.
- Busschers FS, Kasse C, van Balen RT *et al.* 2007. Late Pleistocene evolution of the Rhine-Meuse system in the southern North Sea basin: imprints of climate change, sea-level oscillation and glacio-isostasy. *Quaternary Science Reviews* **26**: 3216–3248.
- Cameron TDJ, Bonny AP, Gregory DM *et al.* 1984. Lower Pleistocene dinoflagellate cyst, foraminiferal and pollen assemblages in four boreholes in the Southern North Sea. *Geological Magazine* **121**: 85–97.
- Cameron TDJ, Bulat J, Mesdag CS. 1993. High resolution seismic profile through a Late Cenozoic delta complex in the southern North Sea. *Marine and Petroleum Geology* **10**: 591–599.
- Cameron TDJ, Crosby A, Balson PS *et al.* 1992. *United Kingdom Offshore Regional Report: the Geology of the Southern North Sea*. HMSO for the British Geological Survey: London.
- Cameron TDJ, Laban C, Schüttenhelm RTE. 1989. Upper Pliocene and Lower Pleistocene stratigraphy in the Southern Bight of the North Sea. In Henriët JP, De Moor D (eds). *The Quaternary and Tertiary Geology of the Southern Bight, North Sea*. Ministry of Economic Affairs Belgian Geological Survey: Ghent.
- Cameron TDJ, Stoker MS, Long D. 1987. The history of Quaternary sedimentation in the UK sector of the North Sea Basin. *Journal of the Geological Society* **144**: 43–58.

- Cartwright J. 1995. Seismic-stratigraphical analysis of large-scale ridge-trough sedimentary structures in the Late Miocene to Early Pliocene of the central North Sea. *Special Publications of the International Association of Sedimentologists* **22**: 285–303.
- Caston VND. 1972. Linear sandbanks in the southern North Sea. *Sedimentology* **18**: 63–78.
- Caston VND. 1977. *Quaternary deposits of the central North Sea, 2: The Quaternary deposits of the Forties field, northern North Sea*. HMSO: London.
- Caston VND, Stride AH. 1970. Tidal sand movement between some linear sand banks in the North Sea off northeast Norfolk. *Marine Geology* **9**: M38–M42.
- Dowdeswell JA, Ottesen D. 2013. Buried iceberg ploughmarks in the early Quaternary sediments of the central North Sea: a two-million year record of glacial influence from 3D seismic data. *Marine Geology* **344**: 1–9.
- Esmerode EV, Lykke-Andersen H, Surlyk F. 2008. Interaction between bottom currents and slope failure in the Late Cretaceous of the southern Danish Central Graben, North Sea. *Journal of the Geological Society* **165**: 55–72.
- Faugères J, Gonthier E, Stow DAV. 1984. Contourite drift molded by deep Mediterranean outflow. *Geology* **12**: 296–300.
- Field ME, Gardner JV, Prior DB. 1999. Geometry and significance of stacked gullies on the northern California slope. *Marine Geology* **154**: 271–286.
- Funnell B. 1996. Plio-Pleistocene palaeogeography of the southern North Sea basin (3.75–0.60 Ma). *Quaternary Science Reviews* **15**: 391–405.
- Fyfe JA, Gregersen U, Jordt H *et al.* 2003. *Oligocene to Holocene*. In *The Millennium Atlas: Petroleum Geology of the Central and Northern North Sea*, Evans D, Graham S, Armour A, Bathurst P (eds). The Geological Society: London; 279–287.
- Galloway WE. 2002. Paleogeographic setting and depositional architecture of a sand-dominated shelf depositional system, Miocene Utsira formation, North Sea Basin. *Journal of Sedimentary Research* **72**: 476–490.
- Garcia M, Parker G. 1989. Experiments on hydraulic jumps in turbidity currents near a canyon-fan transition. *Science* **245**: 393–396.
- Gatliff RW, Richards PC, Smith K *et al.* 1994. *United Kingdom Offshore Regional Report: the Geology of the Central North Sea*. HMSO for the British Geological Survey: London.
- Gee MJR, Gawthrope RL, Bakke K, *et al.* 2007. Seismic geomorphology and evolution of submarine channels from the Angolian continental margin. *Journal of Sedimentary Research* **77**: 433–446.
- Gofędowski B, Nielsen SB, Clausen OR. 2012. Patterns of Cenozoic sediment flux from western Scandinavia. *Basin Research* **24**: 377–400.
- Graham AGC, Stoker MS, Lonergan L *et al.* 2011. *The Pleistocene glaciations of the North Sea basin*. In *Quaternary Glaciations – Extent and Chronology*, 2nd edn, Ehlers J, Gibbard PL (eds). *Developments in Quaternary Science* **15**: 261–298.
- Gyllencreutz R, Backman J, Jakobsson M *et al.* 2006. Postglacial palaeoceanography in the Skagerrak. *The Holocene* **16**: 975–985.
- Harris PT, Whiteway T. 2011. Global distribution of large submarine canyons: geomorphic differences between active and passive continental margins. *Marine Geology* **285**: 69–86.
- Holmes R. 1977. Quaternary deposits of the central North Sea 5. The Quaternary geology of the UK sector of the North Sea between 56° and 58°N. *Report of Institute of Geological Sciences* **77**: 50.
- Huuse M. 2002. Cenozoic uplift and denudation of southern Norway: insights from the North Sea basin. In *Exhumation of the North Atlantic Margin: Timing, Mechanisms and Implications for Petroleum Exploration*, Dore AG, Cartwright JA, Stoker MS, Turner JP, White N (eds). Geological Society, London, Special Publications **196**: 209–233.
- Huuse M, Clausen OR. 2001. Morphology and origin of major Cenozoic sequence boundaries in the eastern North Sea Basin: top Eocene, near-top Oligocene and the mid-Miocene unconformity. *Basin Research* **13**: 17–41.
- Huuse M, Lykke-Andersen H. 2000. Overdeepened Quaternary valleys in the eastern Danish North Sea: morphology and origin. *Quaternary Science Reviews* **19**: 1233–1253.
- Huuse M, Lykke-Andersen H, Michelsen O. 2001. Cenozoic evolution of the eastern Danish North Sea. *Marine Geology* **177**: 243–269.
- Jobe ZR, Lowe DR, Uchytel SJ. 2011. Two fundamentally different types of submarine canyons along the continental margin of Equatorial Guinea. *Marine and Petroleum Geology* **28**: 843–860.
- Kilhams B, McArthur A, Huuse M *et al.* 2011. Enigmatic large-scale furrows of Miocene to Pliocene age from the central North Sea: current-scoured pockmarks? *Geo-Marine Letters* **31**: 437–449.
- Knox RWOB, Bosch JHA, Rasmussen ES *et al.* 2010. Cenozoic. In *Petroleum and Geological Atlas of the Southern Permian Basin Area*, Doornenbal JC, Stevenson AG (eds). EAGE Publications: Houten; 211–223.
- Knudsen KL, Sejrup HP. 1993. Pleistocene stratigraphy in the Devils Hole area, central North Sea: foraminiferal and amino-acid evidence. *Journal of Quaternary Science* **8**: 1–14.
- Knutz PC. 2010. Channel structures formed by contour currents and fluid expulsion: significance for Late Neogene development of the central North Sea basin. *Petroleum Geology Conference Series* **7**: 77–94.
- Komar PD. 1971. Hydraulic jumps in turbidity currents. *Geological Society of America Bulletin* **82**: 1477–1488.
- Kuhlmann G, Langereis CG, Munsterman D *et al.* 2006. Integrated chronostratigraphy of the Pliocene–Pleistocene interval and its relation to the regional stratigraphical stages in the southern North Sea region. *Netherlands Journal of Geosciences* **85**: 29–45.
- Lisiecki LE, Raymo ME. 2005. A Pliocene–Pleistocene stack of 57 globally distributed benthic $\delta^{18}\text{O}$ records. *Paleoceanography* **20**.
- Lisiecki LE, Raymo ME. 2007. Plio-Pleistocene climate evolution: trends and transitions in glacial cycle dynamics. *Quaternary Science Reviews* **26**: 56–69.
- McCave IN. 1971. Sand waves in the North Sea off the coast of Holland. *Marine Geology* **10**: 199–225.
- McMillan AA, Hamblin RJO, Merritt JW. 2005. An overview of the lithostratigraphical framework for the Quaternary and Neogene deposits of Great Britain (onshore). *British Geological Survey Research Report RR/04/04*.
- Miller K, Mountain G, Wright J *et al.* 2011. A 180-million-year record of sea level and ice volume variations from continental margin and deep-sea isotopic records. *Oceanography* **24**: 40–53.
- Mitchum RM, Jr, Vail PR, Thompson S, III. 1977a. Seismic stratigraphy and global changes of sea level, Part 2: The depositional sequence as a basic unit for stratigraphic analysis. In *Seismic stratigraphy – applications to hydrocarbon exploration*, Payton CE (ed.). American Association of Petroleum Geologists Memoir **26**: 53–62.
- Mitchum RM, Jr, Vail PR, Thompson S, III. 1977b. Seismic stratigraphy and global Changes of sea level, Part 6: Stratigraphic interpretation of seismic reflection patterns in depositional sequences. In *Seismic stratigraphy – applications to hydrocarbon exploration*, Payton CE (ed.). American Association of Petroleum Geologists Memoir **26**: 117–133.
- Mulder T, Alexander J. 2001. The physical character of subaqueous sedimentary density flows and their deposits. *Sedimentology* **48**: 269–299.
- Mulder T. 2011. Gravity processes and deposits on continental slope, rise and abyssal plains. In *Deep-Sea Sediments*, Mulder T, HüNeke H (eds). *Developments in Sedimentology* **63**: 25–148.
- Mulder T, Syvitski JPM, Migeon S *et al.* 2003. Marine hyperpycnal flows: initiation, behavior and related deposits. A review. *Marine and Petroleum Geology* **20**: 861–882.
- Nielsen T, Mathiesen A, Bryde-Auken M. 2008. Base Quaternary in the Danish parts of the North Sea and Skagerrak. *Geological Survey of Denmark and Greenland Bulletin* **15**: 37–40.
- Noorbergen LJ, Lourens LJ, Munsterman DK *et al.* 2015. Stable isotope stratigraphy of the early Quaternary of borehole Noordwijk, southern North Sea. *Quaternary International* **386**: 148–157.
- OSPAR. 2000. *Quality Status Report 2000, Region II – Greater North Sea*. OSPAR Commission: London.
- Ottesen D, Dowdeswell JA, Bugge T. 2014. Morphology, sedimentary infill and depositional environments of the Early Quaternary North Sea Basin (56°–62°N). *Marine and Petroleum Geology* **56**: 123–146.
- Otto L, Zimmerman JTF, Furness GK *et al.* 1990. Review of the physical oceanography of the North Sea. *Netherlands Journal of Sea Research* **26**: 161–238.

- Overeem I, Weltje GJ, Bishop-Kay C *et al.* 2001. The Late Cenozoic Eridanos delta system in the southern North Sea Basin: a climate signal in sediment supply? *Basin Research* **13**: 293–312.
- Praeg D. 2003. Seismic imaging of mid-Pleistocene tunnel-valleys in the North Sea Basin – high resolution from low frequencies. *Journal of Applied Geophysics* **53**: 273–298.
- Pratson LF, Coakley BJ. 1996. A model for the headward erosion of submarine canyons induced by downslope-eroding sediment flows. *Geological Society of America Bulletin* **108**: 225–234.
- Pratson LF, Ryan WBF, Mountain GS *et al.* 1994. Submarine canyon initiation by downslope-eroding sediment flows: Evidence in late Cenozoic strata on the New Jersey continental slope. *Geological Society of America Bulletin* **106**: 395–412.
- Rasmussen ES, Vejbæk OV, Bidstrup T *et al.* 2005. Late Cenozoic depositional history of the Danish North Sea Basin: implications for the petroleum systems in the Kraka, Halfdan, Siri and Nini fields. In *Petroleum Geology: North-West Europe and Global Perspectives – Proceedings of the 6th Petroleum Geology Conference*, Doré AG, Vining BA (eds), Petroleum Geology Conferences Ltd. Published by the Geological Society, London 1347–1358.
- Raymo ME. 1994. The initiation of northern hemisphere glaciation. *Annual Review of Earth and Planetary Sciences* **22**: 353–383.
- Rider MH. 2002. *The Geological Interpretation of Well Logs*, 2nd edn. Rider-French Consulting: Sutherland, Scotland.
- Rose J. 2009. Early and Middle Pleistocene landscapes of eastern England. *Proceedings of the Geologists' Association* **120**: 3–33.
- Rundberg Y, Eidvin T. 2005. Controls on depositional history and architecture of the Oligocene-Miocene succession, northern North Sea Basin. *Norwegian Petroleum Society Special Publications* **12**: 207–239.
- Ryan WBF, Carbotte SM, Coplan JO *et al.* 2009. Global multi-resolution topography synthesis. *Geochemistry, Geophysics, Geosystems* **10**: Q03014.
- Sejrup HP, Aarseth I, Ellingsen KL *et al.* 1987. Quaternary stratigraphy of the Fladen area, central North Sea: a multidisciplinary study. *Journal of Quaternary Science* **2**: 35–58.
- Sejrup HP, Aarseth I, Haflidason H. 1991. The Quaternary succession in the northern North Sea. *Marine Geology* **101**: 103–111.
- Sejrup HP, Haflidason H, Aarseth I *et al.* 1994. Late Weichselian glaciation history of the northern North Sea. *Boreas* **23**: 1–13.
- Shepard FP. 1965. Types of submarine valleys: geological notes. *AAPG Bulletin* **49**: 304–310.
- Shepard FP. 1981. Submarine canyons: multiple causes and long-time persistence. *AAPG Bulletin* **65**: 1062–1077.
- Sørensen JC, Gregersen U, Breiner M *et al.* 1997. High-frequency sequence stratigraphy of Upper Cenozoic deposits in the central and southeastern North Sea areas. *Marine and Petroleum Geology* **14**: 99–123.
- Spinelli GA, Field ME. 2001. Evolution of continental slope gullies on the northern California margin. *Journal of Sedimentary Research* **71**: 237–245.
- Stewart MA, Lonergan L, Hampson G. 2013. 3D seismic analysis of buried tunnel valleys in the central North Sea: morphology, cross-cutting generations and glacial history. *Quaternary Science Reviews* **72**: 1–17.
- Stoker MS, Balson PS, Long D *et al.* 2011. *An Overview of the Lithostratigraphical Framework for the Quaternary Deposits on the United Kingdom Continental Shelf*. British Geological Survey Research Report, RR/11/03.
- Stoker MS, Bent A. 1985. Middle Pleistocene glacial and glaciomarine sedimentation in the west central North Sea. *Boreas* **14**: 325–332.
- Stoker MS, Bent AJA. 1987. Lower Pleistocene deltaic and marine sediments in boreholes from the central North Sea. *Journal of Quaternary Science* **2**: 87–96.
- Stoker MS, Praeg D, Hjelstuen BO *et al.* 2005. Neogene stratigraphy and the sedimentary and oceanographic development of the NW European Atlantic margin. *Marine and Petroleum Geology* **22**: 977–1005.
- Stoker MS, Skinner AC, Fyfe JA *et al.* 1983. Palaeomagnetic evidence for early Pleistocene in the central and northern North Sea. *Nature* **304**: 332–334.
- Stow DAV, Mayall M. 2000. Deep-water sedimentary systems: new models for the 21st century. *Marine and Petroleum Geology* **17**: 123–135.
- Stuart JY, Huuse M. 2012. 3D seismic geomorphology of a large Plio-Pleistocene delta – ‘Bright spots’ and contourites in the southern North Sea. *Marine and Petroleum Geology* **38**: 143–157.
- Svendsen E, Sætre R, Mork M. 1991. Features of the northern North Sea circulation. *Continental Shelf Research* **11**: 493–508.
- Syvitski JPM. 1989. On the deposition of sediment within glacier-influenced fjords: oceanographic controls. *Marine Geology* **85**: 301–329.
- Terwindt JHJ. 1971. Sand waves in the Southern Bight of the North Sea. *Marine Geology* **10**: 51–67.
- Turrell WR, Henderson EW, Slessor G *et al.* 1992. Seasonal changes in the circulation of the northern North Sea. *Continental Shelf Research* **12**: 257–286.
- Weirich FH. 1988. Field evidence for hydraulic jumps in subaqueous sediment gravity flows. *Letters to Nature* **332**: 626–629.
- White N, Lovell B. 1997. Measuring the pulse of a plume with the sedimentary record. *Nature* **387**: 888–891.
- Wingfield R. 1990. The origin of major incisions within the Pleistocene deposits of the North Sea. *Marine Geology* **91**: 31–52.
- Wingfield RTR. 1989. Glacial incisions indicating Middle and Upper Pleistocene ice limits off Britain. *Terra Research* **1**: 538–548.
- Wynn RB, Cronin BT, Peakall J. 2007. Sinuous deep-water channels: Genesis, geometry and architecture. *Marine and Petroleum Geology* **24**: 341–387.
- Ziegler PA. 1992. North Sea rift system. *Tectonophysics* **208**: 55–75.